

A 21 MHz Four Square Beam Antenna

Achieving gain on 15 meters within a relatively small space.

The four square beam antenna is a square array of four vertical elements whose radiation pattern can be rapidly switched in direction by altering the relative phases of the four driving currents. The main beam relies on constructive interference of the signals from the elements where the relative phase of each is made up of the phase shift of the driving signal and the phase shift associated with the additional path length due to its spatial separation from the lead element.

At low frequencies where mechanical rotation is difficult for large structures phase control is an attractive possibility and is sometimes used on 80 meters. Typically, though not necessarily, the elements are positioned at the corners of a quarter wavelength square. At 21 MHz the antenna proves to be compact and can be easily accommodated in smaller yards and does not require a tower or a rotator. The array maintains the low angle radiation characteristic of a simple quarter wave vertical monopole but is able to manifest forward gain and reject noise and unwanted transmissions that would otherwise be received outside the main lobe.

This article considers design choices and explains how to design a practical feed system that takes into account the measured interactions between the four elements. The direction control system is also described. Far field measurements are presented that show the switched polar patterns to allow the actual performance to be compared with a theoretical model. A companion article in the September 2013 issue of *QST* presents a practical description of a 21 MHz four square antenna. That article can be found at www.arrl.org/this-month-in-qex.

Design Choices

A design requires a basic decision as to whether the array is to be broadside or diagonally firing; each requires a different set of driving currents. A first order comparison can be made by considering the simple summation of four unit-amplitude plane waves launched with the specified phases from the element locations. See Table 1.

Figure 1 shows the expected polar variations of power gain for broadside and

Table 1

Element Driving Current Phasings Required for Broadside and Diagonal Firing

	NW	NE	SW	SE
Broadside (S Firing)	0	0	-90	-90
Diagonal (NE Firing)	-90	-180	0	-90

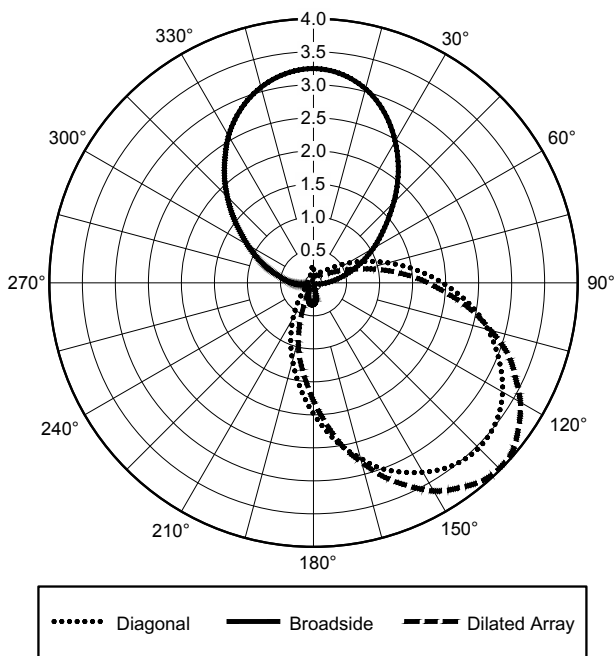


Figure 1 — A simplified comparison of the energy density (P) polar patterns of broadside and diagonally firing four square antennas based on a quarter wavelength square, showing the effect of dilation by a factor of $\sqrt{2}$.

diagonal firing from a quarter-wave square array. Diagonal firing gives about 10% more gain than broadside, but with a half power beamwidth of 90°, wider by 6°. Dilating the square by a factor of $\sqrt{2}$ makes the diagonal length an exact half wavelength and allows waves in that direction to perfectly reinforce. The dashed-line plot shows that this leads to a further increase of gain of about 10% and narrowing of the beamwidth to 84°.

In view of the limited space available, the extra space taken by the enlarged array and its slightly poorer reverse response, I decided to base a design on the smaller diagonally firing array bounded by a quarter-wave square.

The Antenna Array

The array was formed of four quarter wave vertical monopoles, each connected to its own set of quarter wavelength radials lying on the ground. See Figure 2. This basic element of the array was thoroughly characterized and reported in an article in the July 2011 issue of *RadCom*.¹ That study showed that a maximum radiation efficiency of 80% could be achieved with 13 or more ground radials. Purely for convenience, eight radials per monopole were selected for this design, reducing the radiation efficiency to 65%, equivalent to a small eventual loss of 0.9 dB. Figure 3 shows the parallel electrical response of one of the elements in isolation, with no coupling to its neighbors — this was ensured by open circuiting the neighboring driving points.

The design was centered on a frequency of approximately 21.2 MHz using monopole

elements adjusted to be resonant in isolation with a length of 3.34 meters. The side length of the array was 3.55 meters, a quarter wavelength in free space. In order to ensure as far as possible that the coupling between the elements was only electromagnetic, their radial systems were not connected directly to each other; each radial set was returned to its own ground mounting.

It is important to emphasize that because elements in an array interact electromagnetically their properties cannot be

considered to be independent of each other. Currents flowing in a particular element will induce voltages in its neighbors, causing components of current to flow in them and modifying any previously established terminal currents. The coupling between a pair of elements A and B can be expressed through a mutual impedance, Z_{ABm} . Equation 1 calculates the mutual impedance, Z_{ABm} , in terms of the measurements described below.

$$Z_{ABm} = \sqrt{Z_{BB}(Z_{AB} - Z_{AA})} \quad [\text{Eq 1}]$$



Figure 2 — The disposition of the elements, feeders and sets of eight quarter wavelength radials.

¹Notes appear on page 12.

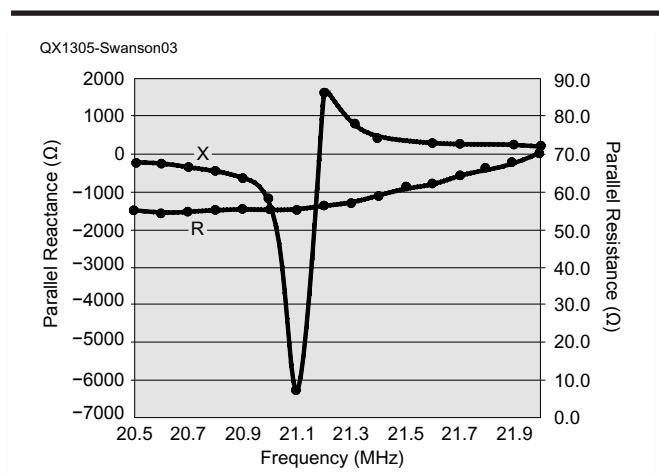


Figure 3 — The parallel electrical response of one of the elements with eight ground level radials when its three neighboring elements were open circuited.

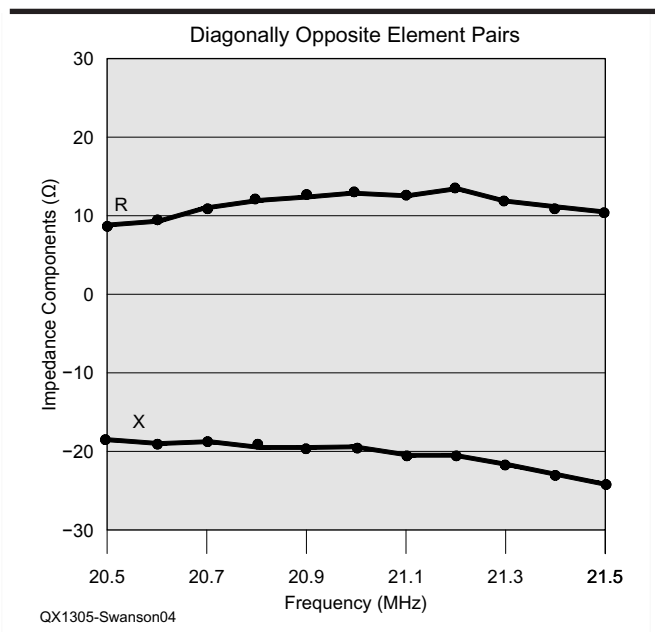


Figure 4 — Averaged measured components of the mutual impedance between pairs of diagonally opposite elements.

The inference of mutual impedances makes use of the principle of superposition, which permits its determination for a particular pair of elements in the absence of the others. As an example, if the mutual impedance between an element A and another element B is to be inferred, the driving point impedance of element A is first measured in isolation with all other driving points open circuited; this gives the value Z_{AA} . Likewise for Z_{BB} . Then Z_{AB} is the impedance of A in the presence of B alone, when the latter is short circuited at its driving point and all other elements are open circuited.

Clearly, coupling to an element A in an array of four requires the determination of Z_{AB_m} , Z_{AC_m} and Z_{AD_m} . A similar statement can be made when element B is considered, and in turn three more values have to be ascertained when each of elements C and D are considered. Three mutual impedance values must be ascertained for each element, a total of 12.

These parameters vary with frequency so the procedure has to be repeated at every frequency at which the mutual impedance is required. Actually the determination of the necessary values is less laborious than it sounds. If the four elements are identical in structure and tested at the same location then $Z_{AA} = Z_{BB} = Z_{CC} = Z_{DD}$ and if pairs A and C and B and D are diagonally opposite, their mutual impedances will be the same. The same reasoning is applicable to the side pairs. So one only needs to measure the isolated impedance values and ascertain the mutual impedances for an edge pair and a diagonally opposite pair. Of course this must be done at each frequency of interest.

The measurements were made with an MFJ-269 Antenna Analyzer remotely connected to the antenna by a length of RG58 coaxial cable, allowing the observer to stand well away from the antenna. The transforming effect of the coaxial cable was removed mathematically by taking into account its characteristic impedance, length, velocity factor and specific attenuation, all of which had been measured independently and found to be: 46 Ω , 10.52 meters, 0.657 and 0.06 dB/m respectively.

A spreadsheet allowed the raw data to be converted into the series elements of driving point impedance. Care was required in order to differentiate between positive(inductive) and negative(capacitive) reactance observations. Measurements were made point by point with frequencies set with an accuracy of ± 10 kHz. Figures 4 and 5 show the inferred components of the mutual impedances for diagonally opposite and edge pairs of elements. These are presented as averaged values; there were relatively small differences between the values obtained for

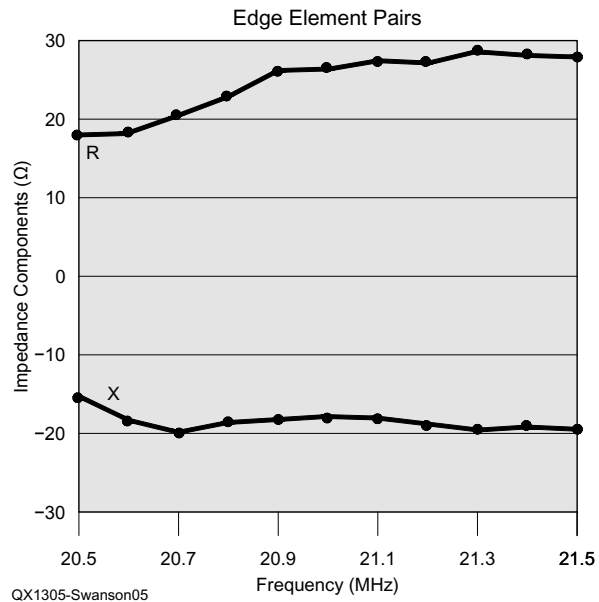


Figure 5 — Averaged measured components of the mutual impedance between pairs of elements at adjacent corners of the array.

particular pairs, perhaps because of small differences in their local environment. I used these averaged values in the design of the RF feed system.

The Feed System

A prerequisite for the design of the feed system of any antenna array is to know the driving point impedance of each element at the frequency of interest when every element is energized. The driving impedance of a particular element is affected by the mutual coupling with all other elements and is related to the mutual impedances by Equation 2, written here for element A.

$$Z_A = Z_{AA} + \frac{i_B}{i_A} Z_{AB_m} + \frac{i_C}{i_A} Z_{AC_m} + \frac{i_D}{i_A} Z_{AD_m} \quad [\text{Eq 2}]$$

Thus the impedance of an element is controlled by the currents in its neighbors, which are set by the required radiation pattern of the array. The problem then becomes how to deliver these currents into the four driving point impedances.

Systems for driving arrays have been reviewed by John Devoldere, ON4UN, in *Low Band DXing*.² A particularly straightforward method that has been chosen here is to make use of a transmission line of an appropriate length to transform the current feeding an antenna element into a voltage that can be preset at the feeder input. The method is sometimes called “current forcing,” because the length of the feeder, the

load impedance and the feeder input voltage completely define the voltage distribution along the feeder and at its termination. It is this terminating voltage that forces the required current to flow into the element driving point. The first step is to calculate the driving point impedances using the four complex currents necessary for a particular radiation pattern.

The four elements have to be individually driven and four separate feeders are needed to provide the transformations that deliver the complex currents required at the driving points. The necessary feeder input voltage will depend on its length. Al Christman, KB8I (now K3LC), pointed out that the feeders, having different lengths, could only be brought together at a common node if the four voltages were equal in magnitude and phase.³ In order to apply the Christman method, we need to be certain that points fulfilling these conditions will actually exist.

Based on the measured impedance parameters at 21.2 MHz, calculations of the four line voltage distributions have been made. Unit currents with the required phase shifts for diagonal firing will have defined the driving point impedances. The complex variations of line voltage are shown in Table 2. It is clear that in this case the magnitude and phase do not match simultaneously at any point. Having applied this method to a broadside firing four square array and a simple two element beam, the Christman method failed in those cases, too. John Devoldere also noted occasional failures of

the Christman method in *Low Band DXing*. See Note 2.

Nevertheless, the method provides a useful basis since points do exist here where the phases match well. These locations along the feeders are highlighted with bold type in Table 2. It requires only transforming the voltages at these equi-phase points to a unique voltage to be able to drive the four feeders from the same source. In this way the equi-phase and equi-voltage conditions would be met. This elaboration of the Christman method is novel and that is what I successfully implemented with my antenna.

Notice that the range of lower feeder lengths, up to 2.4 meters, is not useful because the cables would be too short to reach the four elements from a central point. Notice also that the two central, off axis, feeders require the same current, so only three feeder types are shown in this tabulation.

Table 2 shows the lengths of RG58 feeders that are required to establish the driving point current magnitudes and phase shifts for diagonal firing: they are 3.0 meters for the rear element, 5.2 meters for each of the central elements and 6.9 meters for the leading element. They will deliver the required complex currents to the element driving point impedances, which of course embody the mutual components arising from inter-element coupling. These impedances are shown in Table 3.

This design procedure is a key step in the design of this four square array. The modified Christman method has also been applied successfully to a practical two element design and theoretically to a broadside-firing four square array.

Arranging an Array Common Feed Point

Each element therefore has its own feeder with a length chosen so that it delivers the appropriate complex current to its element and has an input voltage that is in phase with the three other feeder input voltages. Because the feeder input voltage magnitudes differ, it is necessary to transform them to the same voltage, maintaining the same phase so that the array can be fed at a common node. The extent of the voltage adjustment is shown by Table 4.

There is a 3% difference in voltage between the required feeder input voltages for the rear and lead elements. The discrepancy is comparable with the accuracy of the calculations, so these feeder inputs could be simply paralleled. The two central element feeders have the same voltage and phase distributions, so their inputs can be paralleled together. These require a voltage about 20% larger, so scaling down was necessary and an

RF transformer was constructed to do this.

The combined impedance looking into the common feed-point must provide an acceptable match to the 50 Ω line from the transmitter, so not only was voltage scaling required but impedances needed to be scaled too.

An initial attempt to accomplish this using a transformer with two secondary windings was abandoned because it proved

very difficult to neutralize the inductive leakage reactances that were reflected from the secondaries to the primary winding to add to its leakage reactance. Because the two secondary windings shared the same primary winding there was an awkward interaction between the two neutralization steps.

It proved preferable to construct two transformers and to parallel their primary windings. The global leakage

Table 2
Voltage and Phase Along the Three Types of Feeder Showing the Locations of the Equal Phase Points in Bold Type.

Length(meters)	Lead Element Feeder		Central Elements Feeder		Rear Element Feeder	
	Mag	Phase	Mag	Phase	Mag	Phase
0	108.7	-135.5	68.8	-105.8	31.2	-88.2
0.2	112.2	-133.2	66.8	-100.6	24.7	-87.6
0.4	113.8	-131.0	64.1	-95.1	17.8	-86.5
0.6	113.5	-128.9	61.0	-89.0	10.5	-83.9
0.8	111.3	-126.6	57.5	-82.2	3.2	-69.4
1	107.2	-124.3	53.9	-74.4	4.6	75.8
1.2	101.4	-121.6	50.5	-65.6	12.0	84.7
1.4	94.0	-118.6	47.5	-55.5	19.1	86.8
1.6	85.1	-114.9	45.3	-44.2	26.0	87.8
1.8	75.2	-110.4	44.1	-32.0	32.4	88.4
2	64.5	-104.3	44.3	-19.5	38.2	88.8
2.2	53.7	-95.8	45.7	-7.4	43.3	89.2
2.4	43.6	-83.0	48.1	3.7	47.6	89.5
2.6	36.1	-63.9	51.3	13.6	51.0	89.7
2.8	33.5	-38.7	54.9	22.3	53.5	90.0
3	37.2	-14.2	58.6	30.0	55.0	90.3
3.2	45.3	3.7	62.2	36.7	55.6	90.5
3.4	55.6	15.6	65.4	42.8	55.1	90.8
3.6	66.6	23.7	68.0	48.3	53.6	91.2
3.8	77.2	29.5	70.1	53.6	51.2	91.5
4	87.1	33.9	71.4	58.5	47.8	92.0
4.2	95.8	37.6	71.9	63.4	43.5	92.5
4.4	103.1	40.6	71.6	68.3	38.5	93.2
4.6	108.7	43.4	70.6	73.3	32.7	94.2
4.8	112.6	45.9	68.8	78.5	26.4	95.6
5	114.7	48.3	66.4	84.1	19.6	98.0
5.2	114.8	50.7	63.4	90.2	12.6	103.1
5.4	113.1	53.1	60.1	96.9	5.6	121.2
5.6	109.5	55.7	56.6	104.5	4.0	-137.1
5.8	104.2	58.5	53.2	113.1	10.6	-105.8
6	97.2	61.7	50.2	122.8	17.7	-99.0
6.2	88.8	65.5	47.9	133.6	24.6	-96.1
6.4	79.3	70.2	46.6	145.3	31.0	-94.4
6.7	63.7	80.0	46.8	163.4	39.7	-92.9
6.8	58.5	84.4	47.5	169.3	42.2	-92.5
7	48.6	96.1	49.6	-179.5	46.7	-91.8
7.2	40.9	113.1	52.5	-169.4	50.4	-91.2
7.4	37.3	135.4	55.9	-160.5	53.1	-90.6
7.6	39.3	158.7	59.5	-152.6	54.9	-90.1
7.8	46.1	177.4	63.0	-145.6	55.6	-89.6
8	55.5	-169.4	66.3	-139.2	55.4	-89.0
8.2	66.0	-160.2	69.0	-133.4	54.2	-88.5
8.4	76.5	-153.6	71.2	-128.0	51.9	-87.8
8.6	86.4	-148.5	72.6	-122.8	48.8	-87.1
8.8	95.3	-144.4	73.3	-117.8	44.7	-86.2
9	102.8	-140.9	73.2	-112.7	39.9	-85.1
9.2	108.8	-137.9	72.4	-107.6	34.3	-83.7
9.4	113.1	-135.1	70.8	-102.3	28.2	-81.7
9.6	115.5	-132.4	68.6	-96.7	21.6	-78.3
9.8	116.2	-129.8	65.9	-90.6	14.7	-72.0
10	114.9	-127.2	62.7	-84.0	8.1	-54.7

Table 3
Calculated Driving Point Impedances for Diagonal Firing.

Element	Driving Point Impedance (Ω)
Leading	$77.5 + j76.2$
Central(off-axis)	$66.2 - j18.7$
Rear	$1.0 - j\beta 1.1$

reactance of each could be independently neutralized, ensuring that phase shifts in both transformers were zero. The ratio of their secondary turns was determined by the required voltage scaling ratio, in this case, nominally, 0.84. The absolute number of turns in the secondary windings was then determined by the number of primary turns. In practice 20 turns were selected for each transformer because these fit conveniently onto the chosen ferrite toroids. The numbers of secondary turns for the two transformers were then adjusted mathematically to achieve a suitable value for the paralleled primary reflected impedances, always preserving the required ratio between the two secondaries. This procedure led to a common node input impedance of $(51 - j29) \Omega$. The details of the transformers are shown in Table 5.

The transformers were constructed on Type 61 ferrite toroids having an outside diameter of 6 cm and an inside diameter of 4 cm. The primary windings were formed from a single strand of 22 SWG enameled copper wire and the secondaries were of four plaited strands of the same wire wound compactly onto the toroid in the same sense and interleaved with the primary turns. [Note that SWG is British Standard Wire Gauge, with a wire diameter of 0.028 inch. This is roughly equivalent to number 21 American Wire Gauge (AWG), with a diameter of 0.0285 inch. — *Ed.*] Care was taken to begin the ground ends of the two windings at the same position. This helped to minimize the local potential differences between the windings, ensuring that capacitive currents between the windings were minimized. The table shows that more primary turns were required than had been anticipated by a simple view of transformer design. This could be due to winding end effects where the end turns coupled inefficiently to the core. Careful adjustment of the number of turns was made as measurements checked the open circuit voltage ratio. Small errors in achieving the specification are due to an inability to realize fractional turns.

Figure 6 shows the interconnection of the two transformers and the placement of series preset 150 pF neutralizing capacitors. With the secondary short circuited, an oscilloscope was used to observe the primary voltage and current waveforms, and the neutralizing capacitor was adjusted until they

Table 4
Electrical Parameters at the Equal Phase Points.

Position of Feed Point (meters)	Lead Feeder		Central Feeder		Rear Feeder	
	(V)	(degs)	(V)	(degs)	(V)	(degs)
3.0					55.0	90.3
5.2			63.4	90.2		
6.9	53.5	90.3				
Input Z of feeder (Ω)	$16.6 - j15.5$		$46.3 - j21.3$		$21.0 - j161.6$	

Table 5
Details of the Two Transformers Used for Voltage Scaling and Impedance Matching.

	Theoretical Designs		Actual Designs	
	Lead/Rear	Center	Lead/Rear	Center
Primary Turns	20	20	23	23
Secondary Turns	8.4	10	8	10
Combined Input Z	$51 - j29 \Omega$			
OC Voltage Ratio	2.4	2.0	2.3	2.0
	Required	Required	Measured	Measured

Table 6
The Hybrid Ground Electrical Parameters Used for Simulation.

	Relative Permittivity	Electrical Conductivity (S/m)
Inner zone	73	0.75
Outer zone	42	0.088

Table 7
The Actual Drive Currents.

Beam Heading	Measured Elemental Drive Currents (Normalized Magnitude and Phase Angle With Respect to the Rear Element)			
	NE	SE	SW	NW
NE	1.0, -180°	0.67, -90°	1.0, 0°	0.77, -90°
SE	0.93, -105°	1.04, -165°	0.89, -90°	1.0, 0°
SW	1.0, 0°	0.69, -97°	0.97, -192°	0.70, -90°
NW	0.86, -90°	1.0, 0°	0.71, -90°	1.07, -180°

were in phase. The procedure was repeated for the second transformer; there was no interaction between these adjustments. The attenuation of each transformer was about 1.2 dB, equivalent to an efficiency of 76%. The paralleled connection of their primaries provided the driving point of the array.

The actual complex currents flowing into the four elements for the four different beam headings are shown below in Table 7 and discussed later.

The Direction Control System

Figure 7 shows the topology of a switching matrix for routing the three possible phase-shifted feeds to the appropriate elements for a particular direction of fire. The switches used were RF latching reed relays with

a carry current of 1.5 A and a switching time of 2 ms. They were chosen because of their ability to maintain a particular setting without being continuously energized and because they were hermetically sealed and suitable for operation outside. The switches had an actuation current of 16 mA, suitable for control by TTL pull-down devices. This matrix was built on glass-epoxy strip board.

The switch module required five control lines, one to reset the entire switch array and four to select the directions of fire. The direction control lines were routed to the inputs of 2-input NOR gates that energized the appropriate switches for a chosen firing direction. Energy for the switches and NOR gates was supplied by a 9 V battery from a hand held remote controller.

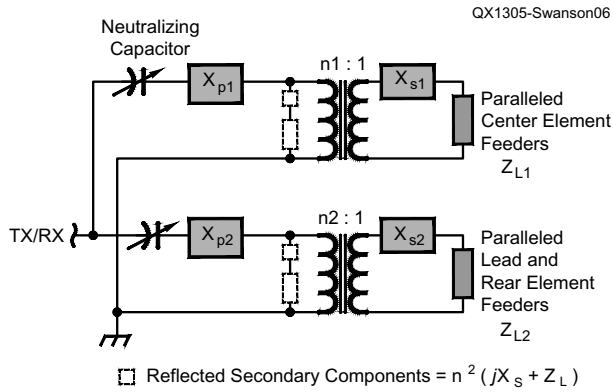


Figure 6 — The interconnection of the feeder transformers.

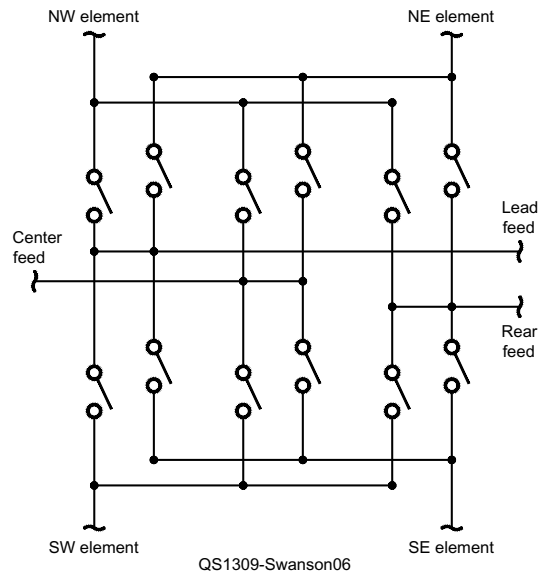


Figure 7 — The router switch array.

QX1305-Swanson08

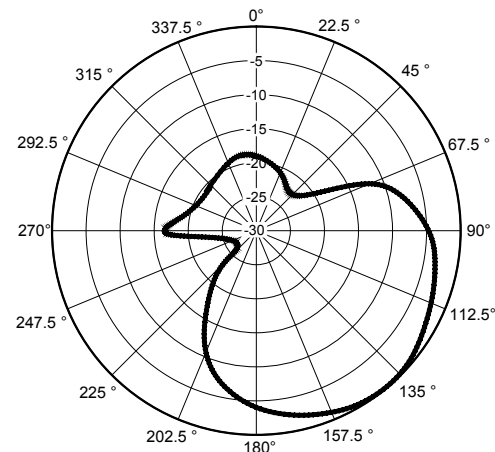
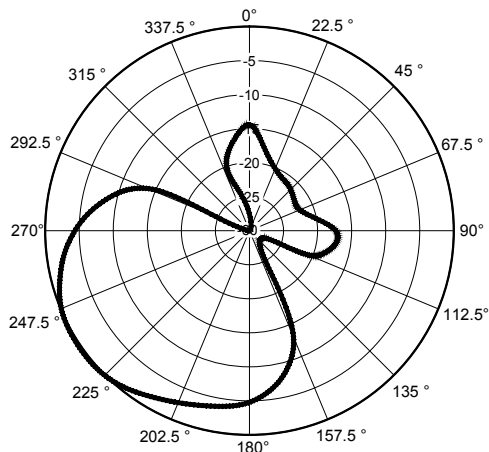
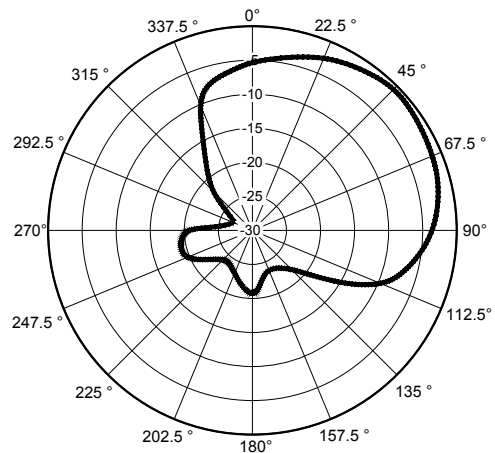
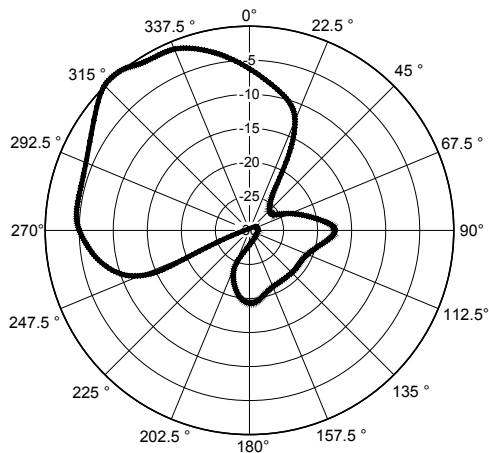


Figure 8 — Measured polar radiation patterns for the four diagonal beam headings.

The antenna design depends critically on transmission lines that have definite lengths, 3.0 meters, 5.2 meters and 6.9 meters. Locating the switching module centrally required that the lengths of the feeders connecting the switch module to the elements should be no less than 2.5 meters, leaving lengths of 0.5 meters, 2.7 meters and 4.0 meters between the module and the common driving point. The latter lengths of feed line were housed with the switch matrix and transformer power splitter modules in a weather-proof box located on the ground centrally between the elements.

The beam is steered by resetting the switches and then briefly energizing the appropriate direction control line to set the required switch configuration. All switching is carried out in the absence of RF excitation to avoid the possibility of contact damage caused by arcing. The system has been in use for two years without any degradation. In principle, the direction of fire could be changed in as little as 4 ms.

The overall measured RF loss from the power splitter output to the elements via the switching matrix was no greater than 0.8 dB and depends slightly on the selected direction. Thus, from the power splitter input to the element inputs there is a loss of about 2 dB, a feed system efficiency of 63%. Since the elements each have a radiation efficiency of about 70% the effective radiation efficiency of the antenna array measured at its feed point is 42%.

Directional Behavior

Polar radiation patterns of an antenna should be measured in the far field of the antenna so that phase differences between signals arriving from parts of the antenna that are off axis are small compared with the phase shifts that would have occurred had they been on the axis. If Δ is the off-axis deviation and R is the range, the phase error in degrees is given by Equation 3.

$$\text{Phase Error (Degrees)} = \frac{180 \Delta^2}{\lambda R} \quad [\text{Eq 3}]$$

The site available for these measurements allowed a range of 38 meters. For this four square array at 21.2 MHz, the maximum phase error at this distance would be no more than 2° . Distortions in the pattern to be measured would therefore be negligible.

Stations were established at 22.5° intervals at a radius of 38 meters from the array center. Measurements were made using a tripod mounted field strength meter with a dynamic range of 90 dB. At each location in turn the received signal — a relative measure of the signal strength — was recorded for each of the four beam headings, with good reproducibility.

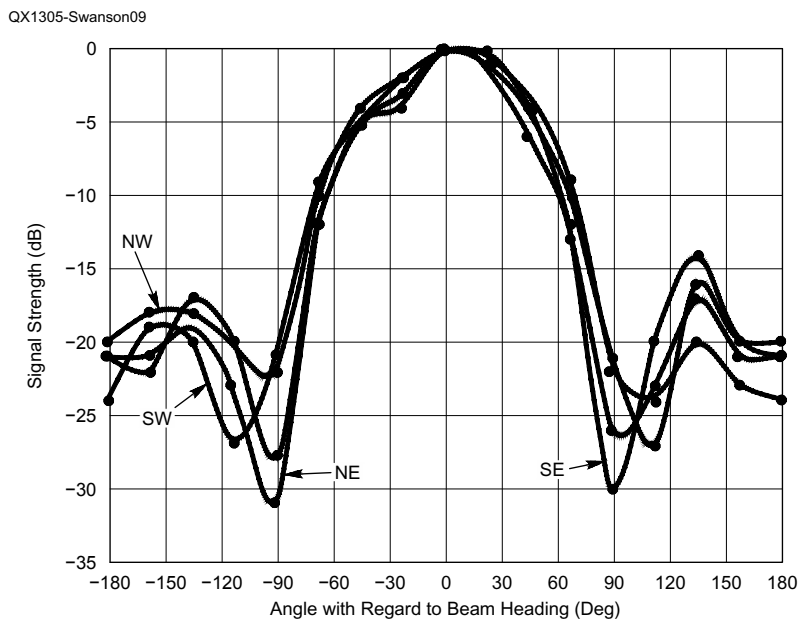


Figure 9 — The four measured patterns overlaid for comparison.

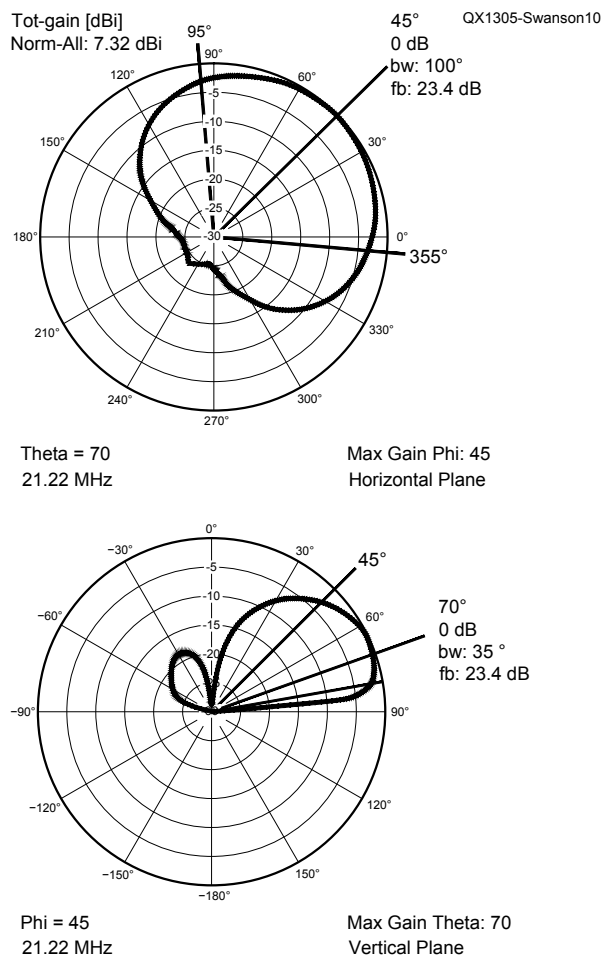


Figure 10 — Computed ideal radiation patterns on the hybrid ground with perfectly defined driving currents.

Figure 8 shows the observed polar patterns for each beam heading. Each is formed from sixteen measured points and data smoothing has been used to help visualize the patterns. Caution is required in interpreting some of the finer angular detail. They are very similar and show clear evidence that switching occurred as intended. They are plots of relative field strength and do not reveal

that the maximum signal strength at each diagonal angle was actually the same, ± 1 dB. The front to back ratio for each pattern was at least 20 dB. These are logarithmic plots, which intrinsically exaggerate detail in the rear sectors; remember that these features are about a hundred times smaller than the main lobes. The half-power beamwidths were about 90° in each case, very close to that

anticipated from a first order analysis earlier in this article. See Figure 1.

Figure 9 represents the superimposed data on rectilinear axes to aid comparison. There is significant and consistent detail in the rear sector. The overall impression is of similarity in the main lobes for the four beam headings.

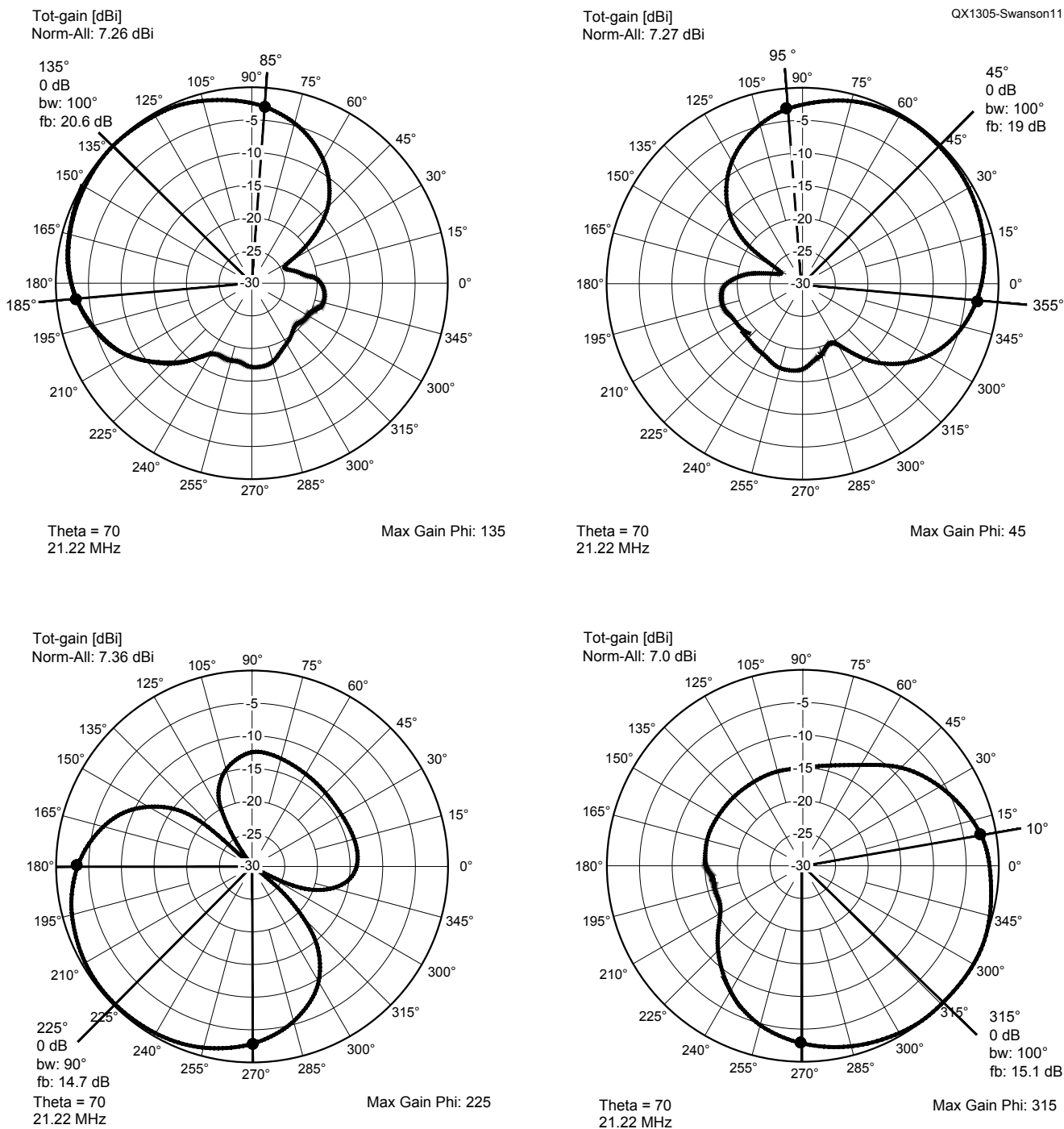


Figure 11 — Computed radiation patterns with the actual driving currents using the hybrid ground. These are all horizontal plane radiation patterns.

Simulation and Modeling

A valid computer model allows experiment and refinement without the effort and time involved in making alterations and new measurements. The *4NEC2* package based on the *NEC2* electromagnetic modeling code offers the advantage of setting current as well as voltage excitations, and is freely available.

The model of the four square antenna that is used here is built on the behavior of independent monopoles, each with their own set of radial wires lying on the ground. This basic unit has been thoroughly characterized and was described in my July 2011 *RadCom* article. See Note 1. Because the *NEC2* code cannot model structures with ground based radial conductors, the ground system has been modeled as a hybrid ground with two concentric ground regions, each with defined electrical parameters. It is convenient that modeling of hybrid concentric grounds is a feature of *4NEC2*.

The electrical parameters of the outer zone, extending to infinity, were obtained by measuring the terminal parameters and resonance frequency of one of the monopoles without any radials at all. Optimization was carried out using the simulator to adjust the ground parameters until the required terminal parameters were obtained. See Note 1.

The central region, a quarter wavelength in radius, is made quasi-metallic by the radials. The optimizer was used again, in this case with the two-zone model, to adjust the parameters of this inner zone until the measured terminal impedance of the element with its eight radials was obtained,

the outer zone parameters being set at the values that had already been determined. The appropriate two-zone parameters for the hybrid ground are stated in Table 6. They represent the behavior of the monopole with eight radials operating at 21.2 MHz on the imperfect ground.

Figure 10 shows the computed behavior of the antenna on the hybrid ground when driven with a perfectly defined set of drive

currents. It provides a basis for comparison when the actual currents were used. The actual complex drive current for each element was measured at each directional setting and used in the simulation to arrive at calculated polar patterns for the four directions, again on the hybrid ground. The normalized currents, which sometimes deviated from the intended values, are listed in Table 7.

The modeled polar patterns using the

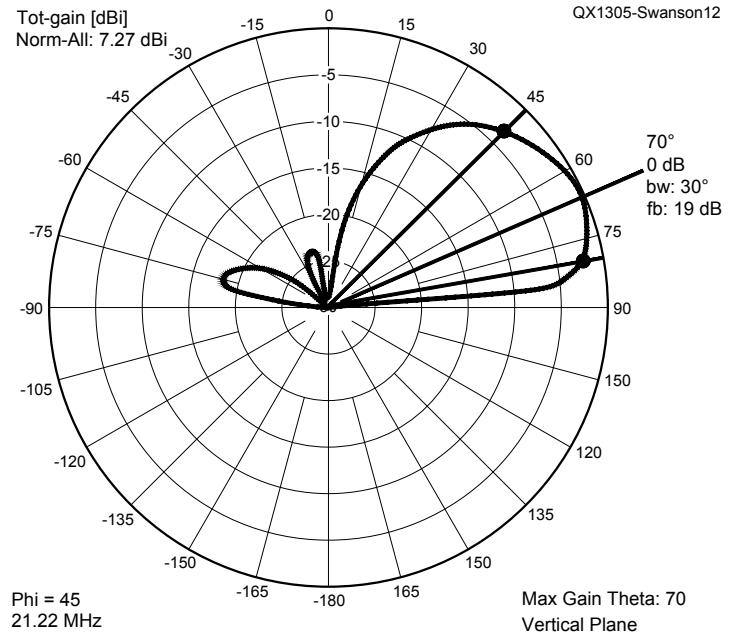


Figure 12 — Computed vertical radiation pattern with the actual driving currents using the hybrid ground.

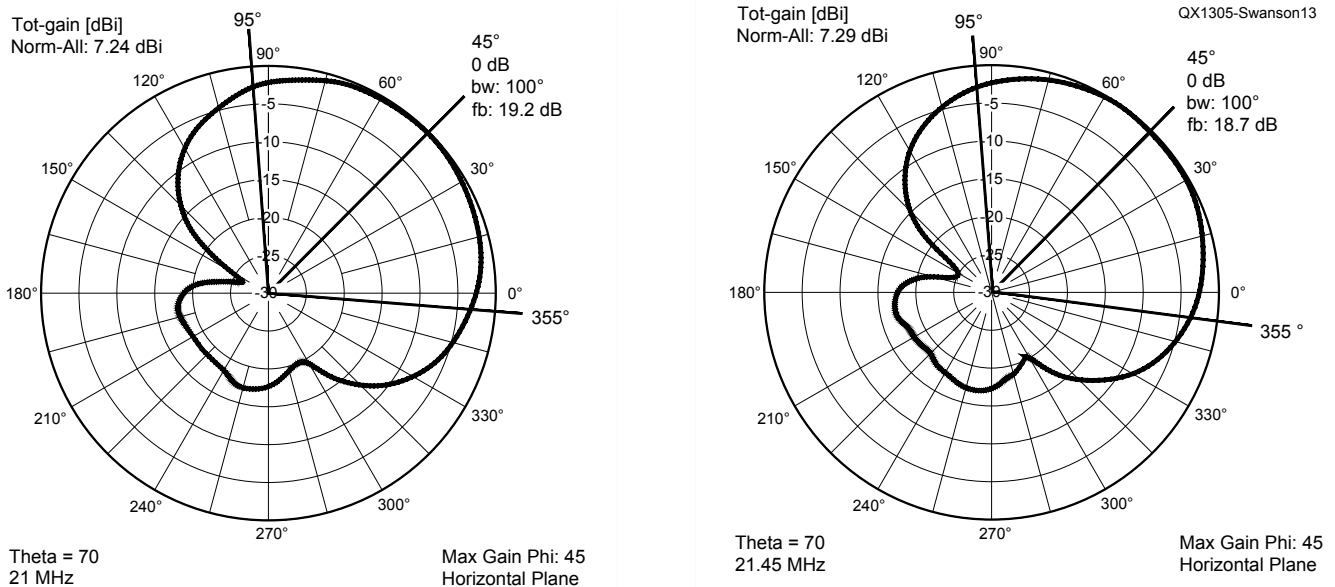


Figure 13 — The computed horizontal radiation patterns at the extremities of the 21 MHz band using the hybrid ground.

actual drive currents are shown in Figure 11. There is good agreement between these and the measured plots shown in Figure 8. The front to back ratios span the range from 20.6 to 14.7 and are somewhat smaller and less consistent than the actual values. See Figure 8. The beamwidths are in very good agreement with the measurements. Predicted, but not measured, are the forward gains; these are very similar for the four directions, ranging between 7.00 and 7.36 dBi.

The simulation also provides the elevation of the main lobe above the horizon. Although the only pattern presented here — Figure 12 — is for the NE direction the elevation is close to 20° for all beam headings, with a half power vertical beamwidth of 35°.

A very useful indication of the insensitivity to frequency as the 21 MHz band was traversed is provided by the two NE polar patterns shown in Figure 13. This 2% change of frequency caused a change of only 0.5 dB in the front to back ratio and a negligible change in gain of only 0.05 dB.

Discussion

The antenna behavior on the hybrid ground, but with a perfect set of drive currents, provides a basis for discussion. See Figure 10, which shows that the forward gain is 7.32 dB, the highest attainable value on this practical ground. The behavior in the rear section is determined by the degree of cancellation of the fields from the four elements. It is here that small differences between the field components become apparent and reflect imperfections in the array and its feed system that result in errors in the drive currents.

Despite the discrepancies between the actual drive currents and those intended, they were used in the simulation and the predicted gain values come close to the maximum attainable on the hybrid ground. Compare Figures 10 and 11. The observed front to back ratios were at least 20 dB on this ground and Figure 10 suggests that an improvement by 3 to 4 dB might be achievable. Although appreciable, it is questionable if this improvement would have practical value when the ratio was already 20 dB. It is interesting to note that with a perfectly defined set of drive currents and a perfect ground the best possible gain and front to back ratio would be 10.8 dBi and 29.8 dB.

In Table 5 the off-axis element drive currents are highlighted. They are invariably low compared with the on-axis elements. It should be relatively easy to correct this by increasing the number of secondary turns of

the appropriate transformer and should lead to an improved front to back ratio. This will undoubtedly disturb the transformation of the central element feeder impedances, however, and measures will be needed to ensure that the transformed impedances combine in parallel to approach 50 Ω.

Harder to understand are the off-axis current asymmetries. These elements are driven from the same secondary winding through two feeders that have the same lengths and should deliver very similar drive currents. The asymmetries are not reversed or replicated when the beam heading is oppositely directed. Had they been due to different local environments for the pair of axis elements the asymmetry would have persisted when the feeders were interchanged, but this did not occur.

No account was taken in the design of the delays introduced by the switching matrix. Although they would be relatively small, the path lengths through the matrix were not equal for the four signals and depended on the pattern of switch closures. It is possible that this is a source of asymmetry and a careful study of these pathways is needed.

There are strong indications from modeling on a practical ground that the forward gain is between 7 and 8 dBi, but this needs to be confirmed by measurement and will require reference to a standard antenna.

Conclusions

An electronically steerable four square phased array antenna has been realized for use at 21 MHz. The antenna has a diagonal fire configuration with a main beam that can be switched rapidly to one of four orthogonal directions. The antenna makes use of a novel feed system that uses two RF transformers to ensure that the element feeders are driven with the same voltage and phase. The overall loss from the array feed point to the element inputs was 2 dB. This elaboration of the Christman method allows it to be used universally in situations where only equi-phase points exist on the set of feeders.

On an imperfect practical ground the antenna achieved a measured front to back ratio in excess of 20 dB — a value consistent with listening and on-air use that showed differences of between 3 and 4 S units. I have not yet measured the forward gain; however, based upon computer modeling using a hybrid model to represent the practical ground, its gain is estimated to be 7 to 8 dBi. The horizontal and vertical half power beamwidths are 90° and 35° respectively with a vertical beam elevation of 20°. Modeling has also predicted that the

antenna characteristics vary only slightly across the operating bandwidth of 0.45 MHz at 21 MHz. The directional properties of the antenna accorded well with computer modeling, which points the way to further improvement.

The performance of another four element beam, the four-element Yagi, provides an interesting comparison. Modeling of the Yagi indicates a gain of 11 dBi, a front-to-back ratio of 20 to 25 dB and a half power beamwidth of 60°.⁴ Practical corresponding values claimed for the four element 21 MHz SteppIR antenna are 10.2 dBi, 27 dB and 60°.⁵

In comparison with the Yagi, the diagonally firing four square antenna at 21 MHz is likely to have a gain 2 to 3 dB lower; it has a similar FB ratio and a half power main beamwidth that is 30° wider. While there is scope for further refinement of this implementation of the four square antenna it is doubtful if the resulting improvements would significantly affect the gain and beamwidth but could improve the observed front-to-back ratio by 3 to 4 dB.

J. Garth Swanson was born in 1941 and obtained a full transmitting license at the age of 16. He graduated from Imperial College London with a BSc (Engineering) in 1963 where he was awarded a PhD in Electrical Engineering in 1967.

He then worked at the Westinghouse Research Laboratory in Pittsburgh, PA for four years, working on thin film electronic devices. On returning to the UK he spent a year in industry and then moved to a career in academia. Garth eventually became chairman of the Electrical Engineering department at King's College in the University of London, where he was a Professor of Physical Electronics with research interests in electronic and optoelectronic materials. He has spent two sabbatical periods at French research laboratories. On his retirement in 2001 he became Professor Emeritus at King's College and has pursued an interest in phased array HF antennas.

Notes

¹Garth Swanson, G3NPC, "The Ground Mounted Quarter Wave Vertical Antenna," *RadCom*, July 2011, pp 60-64.

²John Devoldere, ON4UN, *Low-Band DXing*, 2nd edition, ARRL, 1995.

³Al Christman, KB8I (now K3LC), "Feeding Phased Arrays — An Alternate Method," *Ham Radio*, May 1985, p.58.

⁴ARRL *Antenna Book*, 16th edition, 1991.

⁵SteppIR Antennas Inc, 2112 116th Ave NE, Bellevue, WA, USA. www.steppir.com/4-element-yagi